

Synthesis of terpyridine-containing Pd(II) complexes and evaluation of their catalytic activity

Sanmao Yin, Xiaomin Wang, Jun Jiang, Hongping Xiao, Xinhua Li*

College of Chemistry and Materials Engineering, Wenzhou University, Wenzhou, Zhejiang, 325035, PR China



ARTICLE INFO

Article history:

Received 3 July 2019

Received in revised form

9 August 2019

Accepted 12 August 2019

Available online 14 August 2019

Keywords:

Terpyridine-containing Pd(II) coordination

Crystal structure

Catalyst

Cross-coupling reaction

Triphenylene synthesis

ABSTRACT

Herein, we prepare two terpyridine-containing Pd(II) complexes, $[PdClL_1] \cdot \text{solvent}$ (A_1) and $[PdClL_2] \cdot 2H_2O$ (A_2) ($L_1 = 4'-(4\text{-carboxyl-phenyl})-2,2':6',2''\text{-terpyridine}$, $L_2 = 2,6\text{-bis}(2\text{-pyrazinyl})-4\text{-(4\text{-carboxyl-phenyl})pyridine}$), from $4'-(4\text{-cyanophenyl})-2,2':6',2''\text{-terpyridine}$ (L_{1a})/ $2,6\text{-bis}(2\text{-pyrazinyl})-4\text{-(4\text{-cyanophenyl})pyridine}$ (L_{2a}) and Pd(II) acetate and characterise them by several instrumental techniques. A_1 and A_2 are shown to be good catalysts for the coupling of 2-iodobiphenyl with iodobenzenes to afford triphenylenes, which is known to involve dual C–H bond activation and double C–C bond formation. The obtained data suggest that the mechanism of A_1 -and A_2 -mediated coupling may be similar to the reference Pd catalysts, A_1 and A_2 are also suitable catalysts for this cyclization process. Study on this kind of complexes is of importance to the development of novel Pd-based catalysts and triphenylene synthesis techniques.

© 2019 Elsevier B.V. All rights reserved.

1. Introduction

Multitopic tectons based on [2,2':6',2'']-terpyridine (tpy), a ubiquitous tridentate chelating ligand, have recently attracted increased attention in view of their ability to coordinate diverse metals, facilitating both labile (Zn^{2+} , Cd^{2+}) and non-labile (Ru^{2+} , Os^{2+}) tpy-M $^{2+}$ -tpy connectivity and thus permitting control over bond strength and, ultimately, over molecular architecture [1]. Consequently, pseudo-octahedral tpy-M $^{2+}$ -tpy moieties were widely employed as monomers of diverse metalloendrimers [2], racks [3], and grids [4], and were also popular components of macrocycles, cages, and diverse polyhedra [5]. Moreover, the unique structure and properties of terpyridine-based functional complexes have been used in the fields of optics [6–10], magnetic material synthesis [11,12], supramolecular chemistry [13,14], biochemistry [15], catalysis [16,17], and anticancer drug design [18,19].

Pentacoordinated polypyridyl Cu(II) coordination complexes can efficiently cleave DNA [20–23], while square planar Pt-terpyridine complexes are very good G-quadruplex binders [24–28]. However, despite the abundance of functional complexes comprising terpyridine-based monomers and the large variety of

available stepwise assembly processes, seldom Pd $^{2+}$ -terpyridine complexes have been reported to date [29–33]. Herein, we describe the synthesis, characterization, and catalytic activity of two functional complexes of Pd $^{2+}$ containing $4'-(4\text{-carboxyl-phenyl})-2,2':6',2''\text{-terpyridine}$ (L_1) and $2,6\text{-bis}(2\text{-pyrazinyl})-4\text{-(4\text{-carboxylphenyl})pyridine}$ (L_2) (Scheme 1). The square planar Pd $^{2+}$ -terpyridine complexes are very good cross-coupling catalysts.

Complexes A_1 and A_2 were separately prepared using $4'-(4\text{-cyanophenyl})-2,2':6',2''\text{-terpyridine}$ (L_{1a}) and $2,6\text{-bis}(2\text{-pyrazinyl})-4\text{-(4\text{-cyanophenyl})pyridine}$ (L_{2a}) as precursor ligands and Pd(II) acetate ($Pd(OAc)_2$) as a Pd source, and the structures of these complexes were probed by several instrumental techniques. Moreover, we investigated the ability of A_1 and A_2 to catalyse the formation of triphenylene via C–C coupling of 2-iodobiphenyl with iodobenzenes.

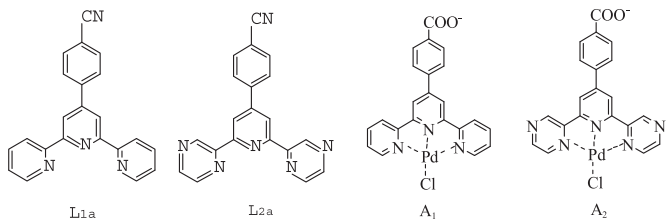
2. Results and discussion

2.1. Structural characterization

Fig. S1 shows the experimental and simulated powder XRD patterns of A_1 . The experimental and simulated patterns were in good agreement, which indicated that the title compound featured one homogeneous phase. TGA of L_{1a} and A_1 (Fig. S2) showed that the latter was more thermally stable than the former, i.e., A_1 was confirmed to be a coordination complex of Pd. The observation of

* Corresponding author.

E-mail address: lixinhua01@126.com (X. Li).



Scheme 1. Structures of complexes A₁, A₂ and precursor ligands L_{1a} and L_{2a}.

C–O (1399–1608 cm^{−1}) and C=O (1696.6 cm^{−1}) bands in the FT-IR spectrum of A₁ (Fig. S3) demonstrated that A₁ comprised Pd ions and 4'-(4-carboxyl-phenyl)-2,2':6',2''-terpyridine (L₁), i.e., the –CN group was converted into a –COO[−] group [34]. In support of this assumption, the C=O band was blue-shifted because of the conjugation between the carboxyl group and the benzene ring. The absence of characteristic –COOH bands at 1710 cm^{−1} indicated that carboxylate groups in A₁ were completely deprotonated, as was further confirmed by single-crystal XRD.

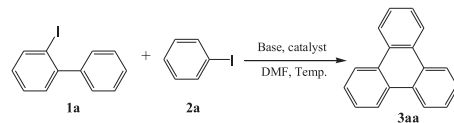
Single-crystal XRD analysis revealed that A₁ crystallised in the monoclinic C₂/c space group and featured a structural unit containing one crystallographic Pd²⁺ ion, one L₁ ligand, and one Cl[−] anion (Fig. 1). Each Pd²⁺ ion exhibited a distorted square-planar geometric configuration and was coordinated by Cl[−] (Cl1) and three nitrogen atoms (N1, N2, and N3) of the terpyridine moiety of L₁. Thus, the Pd²⁺ ion was coordinatively unsaturated, which was of key importance for the catalytic activity of A₁. L₁ acted as a tridentate ligand, and its carboxylate group was non-coordinated but deprotonated to achieve charge balance. Pd–N bond lengths lied in the range of 1.929(6)–2.016(7) Å. The torsion angle between the phenyl and the terpyridine planes was 37.53(8) degree, and the torsion angle between the carboxylate and the phenyl was 174.61(7) degree. The structure of A₂ was found to be similar to that of A₁ (Figs. S4–S6). The Pd–Cl bond lengths in A₁ and A₂ were 2.284(2) Å and 2.025 (3) Å, respectively.

2.2. Dual C–H bond activation and double C–C bond formation

There has been ongoing interest in the development of triphenylenes [35], as triphenylenes were widely employed to prepare functional organic materials such as discotic liquid crystals and organic light-emitting diodes [36–39]. Among the variety of triphenylene synthesis strategies, those based on Pd catalysis have gained great attention, offering ease of implementation and high efficiency [40]. However, C–C coupling catalysed by Pd-terpyridine

complexes has seldom been reported yet.

Since triphenylenes can be synthesised from readily available 2-iodobiphenyls and iodobenzenes under the conditions of Pd catalysis [41], we attempted to employ A₁ and A₂ as catalysts of the cross-coupling reaction between 2-iodobiphenyl and iodobenzenes under mild conditions without the use of expensive and toxic dppf ligand and a protective N₂ atmosphere. To our delight, the reaction of 2-iodobiphenyl with iodobenzene catalysed by A₁ ([PdClL₁]·solvent) and A₂ ([PdCl₂]·2H₂O) in dimethylformamide (DMF) under mild conditions afforded triphenylene in isolated yields of 34 and 22%, respectively (Table 1, entry 1). The obtained product was characterised by NMR, and its physical and spectral data were compared to those reported in literature (Fig. S7) [41]. The above coupling reaction was used to determine the optimal reaction conditions. First, we investigated the effect of catalyst loading (Table 1), showing that the highest yield was obtained at 10 at% A₁ or A₂, with A₁ featuring a higher catalytic activity than A₂. Hence, subsequent experiments were performed with 10 at% A₁.



Second, we probed the effect of base type/loading, revealing that although strong bases were more effective than weak bases, decreased yields were observed for very strong bases (Table 2, entry 2). As has been described in literature [41], the highest yield was obtained in the presence of Na₂CO₃ and CsOAc (entry 1). Finally, we optimised reaction time, temperature, and solvent, and the optimum reaction conditions were identified as iodobenzene (2 equiv), 2-iodobiphenyl (1 equiv), Na₂CO₃ (2 equiv), CsOAc (3 equiv), A₁ or A₂ (10 at%) in DMF at 120 °C.

Having developed an efficient procedure for the synthesis of triphenylene, we investigated the corresponding substrate scope. As A₁ featured a higher catalytic activity than A₂, only the former catalyst was employed in the following reactions.

Table 1
Effect of catalyst loading on triphenylene yield.

Entry	Catalyst (mmol%)	Product (A ₃)	yield A ₁ (%)	yield A ₂ (%)
1	5	3aa	34.2	22(0.5 ^a)
2	10	3aa	50.8	38(0.8)
3	15	3aa	45.4	26(0.6)

^a Margins of error for multiple experiments.

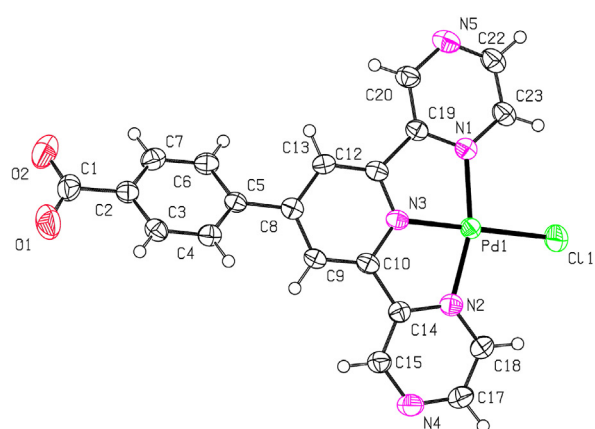
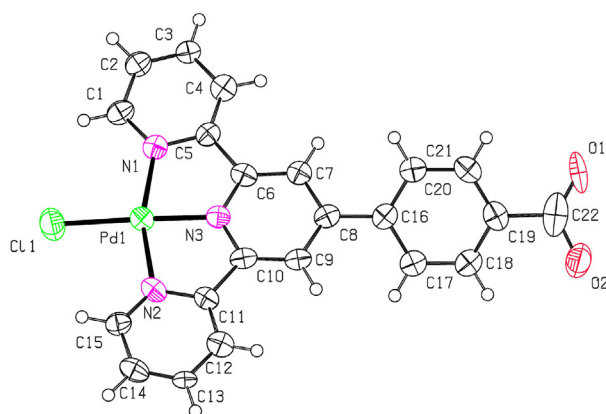


Fig. 1. Coordination environment of Pd(II) in A₁ (left) and A₂ (right), with displacement ellipsoids drawn at the 30% probability level.

Table 2
Effect of base type and loading on triphenylene yield.

Entry	Base	Yield(%)
1	Na ₂ CO ₃ (2equiv) + CsOAc(3equiv)	51(0.6)
2	NaOH(4equiv) + CsOAc(3equiv)	38(0.9)
3	Na ₂ CO ₃ (2equiv) + Cs ₂ CO ₃ (1.5equiv)	trace
4	Cs ₂ CO ₃ (3.5equiv)	trace

Table 3 lists the results obtained when several iodobenzenes were coupled with 2-iodobiphenyl to assess the catalytic activity of A₁. Notably, 2-iodobiphenyl smoothly reacted with most iodobenzene derivatives to afford triphenylenes in moderate to good yields, and iodobenzenes bearing electron-withdrawing groups were found to be more reactive than those with electron-withdrawing groups. Both chloro and fluoro groups were tolerated (entries

6–8), and reactions of iodobenzenes containing *m*- or *p*-methyl groups furnished the same product, **3gg** (entries 7 and 8). The reactions of iodobenzenes bearing electron-withdrawing groups such as CF₃ and Cl were low-yielding (entries 5 and 7), which was mainly ascribed to the large extent of concomitantly occurring homocoupling to form biphenyl byproducts. In fact, the yield of triphenylenes could be improved in all cases when iodobenzenes were used in excess. While the detailed mechanism of the catalysis reaction remains to be investigated and other reaction pathways cannot be ruled out, based on our previous works and reference [41], a similar tentative mechanism was proposed as shown in [Supporting Information](#).

3. Material and methods

3.1. Chemicals

All chemicals (AR grade) were obtained from commercial sources and used without further purification. Petroleum ether refers to the fraction with a boiling point of 60–90 °C. Reaction progress was monitored by thin layer chromatography (silica gel, Polygram SILG/UV 254 plates). Column chromatography was performed using Silicycle silica gel (200–300 mesh).

3.2. Preparation of A₁ and A₂

Pd(OAc)₂ and (0.205 g, 1 mmol) was dissolved in HOAc (3 mL) to afford solution A, while L_{1a}/L_{2a} (0.336 g, 1 mmol/0.334 g, 1 mmol) was suspended in pure water (15 mL) at room temperature to afford solution B. Subsequently, solution A was dropwise added to solution B, and the resulting mixture was treated with 30 wt% HCl (2 mL) and stirred for 30 min to afford a light red suspension. The suspension was transferred to a polytetrafluoroethylene (PTFE)-lined 50-mL stainless steel reactor and heated to 150 °C at a rate of 10 °C h⁻¹. The above temperature was maintained for 72 h, and the reactor was then cooled to room temperature at a rate of 5 °C h⁻¹. The product was washed with 10 wt% sodium hydroxide solution to furnish light red acicular crystals (0.170 g/0.166 g, yield = 83%/81% based on Pd(OAc)₂) that were dried at 100 °C overnight.

3.3. Characterization

Melting points (uncorrected) were determined on an Omega MPS10 digital melting point apparatus. ¹H and ¹³C NMR spectra were recorded on a Bruker DRX-500 (500 MHz) spectrometer in CDCl₃ using tetramethylsilane (TMS) as an internal reference. All chemical shifts were reported relative to that of TMS (0.0 ppm). All compounds (known and unknown) were identified by ¹H and ¹³C NMR. The physical and spectral data of known compounds were compared with those reported in literature. Single-crystal X-ray diffraction (XRD) patterns were recorded on a Bruker Smart-1000 CCD diffractometer, while powder XRD measurements were performed on a Bruker D8 Advance diffractometer at 40 kV and 40 mA using Cu K_α ($\lambda = 15.406 \text{ nm}$) radiation, a scan step of 0.01°, and a scan speed of 0.1 s step⁻¹. Thermogravimetric analysis (TGA) was performed under N₂ at a heating rate of 5 °C min⁻¹ using a TA-Q600 system (TA Instruments, USA). The thermal stability of the synthesised complex precursor was investigated in the range between ambient temperature and 800 °C. Fourier transform infrared (FT-IR) spectra were recorded on a Thermo Scientific Nicolet iS10 spectrometer in the range of 4000–400 cm⁻¹ using the KBr pellet technique. Elemental analyses (C and H) were carried out on a Carlo-Erba 1112 Elemental Analyzer.

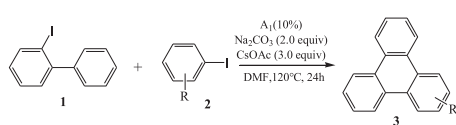


Table 3
Results of C–C coupling reactions catalysed by A₁.

Entry	Substrate(2a)	Product	Yield(%)
1			71(0.6)
2			73(0.2)
3			56 (0.3)
4			31(0.8)
5			49(0.7)
6			53 (0.6)
7			39(1.0)
8			45 (0.9)

Unless otherwise noted, the following conditions were used: **1**: 0.2 mmol, **2**: 0.4 mmol, catalyst: 10 at%, Na₂CO₃: 2.0 equiv, CsOAc: 3.0 equiv, DMF: 3 mL, 120 °C, 24 h.

3.4. General experimental procedure for the catalytic coupling of 2-iodobiphenyl with iodobenzenes

A tubular reactor was charged with Na_2CO_3 (0.0424 g, 0.4 mmol), CsOAc (0.1152 g, 0.6 mmol), 2-iodobiphenyl (0.0560 g, 0.2 mmol), iodobenzene (0.0816 g, 0.4 mmol), A_1 (10 at%), and solvent (3 mL), sealed, and heated to 120 °C in an oil bath for 24 h. Subsequently, the reaction mixture was cooled and quenched with brine (20 mL) and ethyl acetate (40 mL). The organic layer was retained, and the aqueous phase was extracted with ethyl acetate (2×40 mL). All organic phases were combined, dried over anhydrous MgSO_4 , and filtered. The desired product was separated via vacuum distillation and was further purified by silica gel thin layer chromatography using petroleum ether as an expansion agent. The product-containing silica gel was scraped off and pulverised. The powder was leached with ethyl acetate for 4 h, and the leachate was filtered and subjected to vacuum distillation.

4. Conclusions

In conclusion, we prepared and characterised $\text{Pd}(\text{II})$ -terpyridine coordination complexes A_1 and A_2 , showing that they effectively catalyse the cross-coupling of iodobenzenes and 2-iodobiphenyl to afford asymmetrically functionalised triphenylenes. The square-planar and unsaturated Pd^{2+} ion of Pd^{2+} -terpyridine complexes play key role for their catalysis properties. The above reaction is thought to involve two Pd -catalysed C–H bond activations and two Pd -catalysed C–C bond formation steps, and thus offers high atom and step economy. Contrary to previously reported Pd -based catalysts, the complexes described herein do not require the use of toxic dppf as a ligand and a protective N_2 atmosphere. Therefore, this study reports another catalyst for this cyclization process and it is valuable to the development of novel routes to polycyclic aromatic hydrocarbons. Further investigations aimed at elucidating the detailed mechanism of the described reaction and improving its yield are currently underway in our laboratory.

Notes

The authors declare no competing financial interest.

Acknowledgements

We gratefully acknowledge financial support provided by the National Natural Science Foundation of China (grant numbers 21571144).

Appendix A. Supplementary data

Supplementary data to this article can be found online at <https://doi.org/10.1016/j.molstruc.2019.126925>.

References

- [1] S. Chakraborty, G.R. Newkome, Terpyridine-based metallosupramolecular constructs: tailored monomers to precise 2D-motifs and 3D-metallocages, *Chem. Soc. Rev.* 47 (2018) 3991–4016.
- [2] J.L. Wang, X. Li, C.D. Shreiner, X. Lu, C.N. Moorefield, S.R. Tummala, D.A. Medvetz, M.J. Panzner, F.R. Fronczek, C. Wesdemiotis, G.R. Newkome, Shape-persistent ruthenium(II)-and iron (II)-bisterpyridine metallocodrimers: synthesis, traveling-wave ion-mobility mass spectrometry, and photophysical properties, *New J. Chem.* 36 (2012) 484–491.
- [3] G.S. Hanan, C.R. Arana, J.M. Lehn, D. Fenske, Synthesis, structure, and properties of dinuclear and trinuclear rack-type rull complexes, *Angew. Chem. Int. Ed.* 34 (1995) 1122–1124.
- [4] M. Barboiu, G. Vaughan, R. Graff, J.M. Lehn, Self-assembly, structure, and dynamic interconversion of metallosupramolecular architectures generated by $\text{Pb}(\text{II})$ binding-induced unfolding of a helical ligand, *J. Am. Chem. Soc.* 125 (2003) 10257–10265.
- [5] T.Z. Xie, Y. Yao, X. Sun, K.J. Endres, S. Zhu, X. Wu, H. Li, J.M. Ludlow, T. Liu, M. Gao, C.N. Moorefield, M.J. Saunders, C. Wesdemiotis, G.R. Newkome, Supramolecular arrays by the self-assembly of terpyridine-based monomers with transition metal ions, *Dalton Trans.* 47 (2018) 7528–7533.
- [6] J. Zhang, W. Yang, X.Y. Wu, Synthesis, photoluminescence, and gas adsorption properties of a new furan-functionalized MOF and direct carbonization for synthesis of porous carbon, *Cryst. Growth Des.* 15 (2016) 475–482.
- [7] M.R.E. da Silva, T. Auvray, B. Laramée-Milette, M.P. Franco, A.A.C. Braga, H.E. Toma, G.S. Hanan, Unusual photooxidation of s-bonded mercaptopyridine in a mixed ligand ruthenium(II) complex with terpyridine and bipyridine ligands, *Inorg. Chem.* 57 (2018) 4898–4905.
- [8] P. Pal, S. Mukherjee, D. Maity, S. Baitalik, Synthesis, structural characterization, and luminescence switching of diarylethene-conjugated $\text{ru}(\text{II})$ -terpyridine complexes by trans-cis photoisomerization: experimental and DFT/TD-DFT investigation, *Inorg. Chem.* 57 (2018) 5743–5753.
- [9] A. Schiffrin, M. Capsoni, G. Farahi, C.G. Wang, C. Krull, M. Castelli, T. Roussy, K.A. Cochrane, Y. Yin, N.V. Medhekar, M. Fuhrer, A.Q. Shaw, W. Ji, S.A. Burke, Designing optoelectronic properties by on-surface synthesis: formation and electronic structure of an iron-terpyridine macromolecular complex, *ACS Nano* 12 (2018) 6545–6553.
- [10] Y. Luo, M. Wächtler, K. Barthelmes, A. Winter, U.S. Schubert, B. Dietzek, Direct detection of the photoinduced charge-separated state in a $\text{Ru}(\text{II})$ bis(terpyridine)- polyoxometalate molecular dyad, *Chem. Commun.* 54 (2018) 2970–2973.
- [11] S.M. Munzert, G. Schwarz, D.G. Kurth, Kinetic studies of the coordination of mono- and ditopic ligands with first row transition metal ions, *Inorg. Chem.* 55 (2016) 2565–2573.
- [12] D. Zych, A. Slodek, M. Matussek, 4-Phenyl-2,2':6,2"-terpyridine derivatives-synthesis, potential application and the influence of acetylene linker on their properties, *Dyes Pigments* 146 (2017) 331–343.
- [13] M. Chen, J. Wang, D. Liu, Z. Jiang, Q. Liu, T. Wu, H. Liu, W. Yu, J. Yan, P. Wang, Highly stable spherical metallo-capsule from a branched hexapodal terpyridine and its self-assembled berry-type nanostructure, *J. Am. Chem. Soc.* 140 (2018) 2555–2561.
- [14] D. Liu, H. Liu, B. Song, M. Chen, J. Huang, J. Wang, X. Yang, W. Sun, X. Li, P. Wang, Terpyridine-based metallo-organic cages and supramolecular gelation by coordination-driven self-assembly and host-guest interaction, *Dalton Trans.* 47 (2018) 14227–14232.
- [15] Q.P. Qin, T. Meng, M.X. Tan, Y.C. Liu, S.L. Wang, B.Q. Zou, H. Liang, Synthesis, characterization and biological evaluation of six highly cytotoxic ruthenium(III) complexes with 4'substituted-2,2'6'2"-terpyridine, *Med. Chem. Commun.* 9 (2018) 525–533.
- [16] M. Clemente-León, E. Coronado, C. Martí-Gastaldo, F.M. Romero, Multi-functionality in hybrid magnetic materials based on bimetallic oxalate complexes, *Chem. Soc. Rev.* 40 (2011) 473–497.
- [17] Z. Lin, N.C. Thacker, T. Sawano, T. Drake, P. Ji, G. Lan, L. Cao, S. Liu, C. Wang, W. Lin, Meta-organic layers stabilize earth-abundant metal-terpyridine diradical complexes for catalytic C–H activation, *Chem. Sci.* 9 (2018) 143–151.
- [18] Q. Cao, Y. Li, E. Freisinger, P.Z. Qin, R.K.O. Sigel, Z.W. Mao, G-quadruplex DNA targeted metal complexes acting as potential anticancer drugs, *Inorg. Chem. Front.* 4 (2017) 10–32.
- [19] M.M. Milutinović, Ž.D. Bugarčić, R. Wilhelm, A camphor based 1,3-diamine $\text{Ru}(\text{II})$ terpyridine complex: synthesis, characterization, kinetic investigation and DNA binding, *New J. Chem.* 42 (2018) 7607–7611.
- [20] J.W. Liang, Y. Wang, K.J. Du, G.Y. Li, R.L. Guan, L.N. Ji, H. Chao, Synthesis, DNA interaction and anticancer activity of copper(II) complexes with 4'-phenyl-2,2':6,2"-terpyridine derivatives, *J. Inorg. Biochem.* 141 (2014) 17–27.
- [21] K. Suntharalingam, D.J. Hunt, A.A. Duarte, A.J.P. White, D.J. Mann, R. Vilar, A tri-copper(II) complex displaying DNA-cleaving properties and anti-proliferative activity against cancer cells, *Chem. Eur. J.* 18 (2012) 15133–15141.
- [22] M. Wehbe, A.W.Y. Leung, M.J. Abrams, C. Orvig, M.B. Ballya, A perspective-can copper complexes be developed as a novel class of therapeutics? *Dalton Trans.* 46 (2017) 10758–10773.
- [23] K. Tummala, C.S. Vasavi, P. Munusami, M. Pathak, M.M. Balamurali, Evaluation of DNA/protein interactions and cytotoxic studies of copper(II) complexes incorporated with N,N donor ligands and terpyridine ligand, *Int. J. Biol. Macromol.* 95 (2017) 1254–1266.
- [24] A. Maroń, K. Czerwińska, B. Machura, L. Raposo, C. Roma-Rodrigues, A.R. Fernandes, J.G. Malecki, A. Szlapa-Kula, S. Kula, S. Krompiec, Spectroscopy, electrochemistry and antiproliferative properties of $\text{Au}(\text{III})$, $\text{Pt}(\text{II})$ and $\text{Cu}(\text{II})$ complexes bearing modified 2,2':6,2"-terpyridine ligands, *Dalton Trans.* 47 (2018) 6444–6463.
- [25] H. Bertrand, D. Monchaud, A.D. Cian, R. Guillot, J.L. Mergny, M.P. Teulade-Fichou, The importance of metal geometry in the recognition of G-quadruplex-DNA by metal-terpyridine complexes, *Org. Biomol. Chem.* 5 (2007) 2555–2559.
- [26] S. Gama, I. Rodrigues, F. Mendes, I.C. Santos, E. Gabano, B. Klejevskaja, J. González-García, M. Ravera, R. Vilar, A. Paulo, Anthracene-terpyridine metal complexes as new G-quadruplex DNA binders, *J. Inorg. Biochem.* 160 (2016) 275–286.
- [27] L. Ronconi, C. Marzano, P. Zanello, M. Corsini, G. Miolo, C. Macca, A. Trevisan, D. Fregona, Gold(III) dithiocarbamate derivatives for the treatment of cancer: solution chemistry, DNA binding, and hemolytic properties, *J. Med. Chem.* 49

- (2006) 1648–1657.
- [28] V. Milacic, Q.P. Dou, The tumor proteasome as a novel target for gold(III) complexes implications for breast cancer therapy, *Coord. Chem. Rev.* 253 (2009) 1649–1660.
- [29] I. Eryazici, C.N. Moorefield, G.R. Newkome, Square-planar Pd(II), Pt(II), and Au(III) terpyridine complexes: their syntheses, physical properties, supramolecular constructs, and biomedical activities, *Chem. Rev.* 108 (2008) 1834–1895.
- [30] A.J. Blake, C. Caltagirone, V. Lippolis, M. Shamsipur, A new polymorph of poly [bis(μ_2 -perchlorato- $\kappa^2O:O'$)(2,2':6',2"-terpyri-dine- κ^3N,N',N'')lead(II)] with a greatly extended chain repeat distance, *Acta Crystallogr. C* 65 (2009) m33–m36.
- [31] S. Perera, X. Li, M. Soler, A. Schultz, C. Wesdemiotis, C.N. Moorefield, G.R. Newkome, Hexameric palladium(II) terpyridyl metallamacrocycles: assembly with 4,4'-Bipyridine and characterization by TWIM mass spectrometry, *Angew. Chem. Int. Ed. Engl.* 49 (2010) 6539–6544.
- [32] S.I. Büyükekş, E. Erkisa, A. Şengül, E. Ulukaya, A.Y. Oral, Structural studies and cytotoxic activity of a new dinuclear coordination compound of palladium(II)-2,2':6',2"-terpyridine with rigid dianionic 1,2,4-triazole-3-sulfonate linker, *Appl. Organomet. Chem.* 32 (2018), e4406.
- [33] Z. Ou, Y. Qian, Y. Gao, Y. Wang, G. Yang, Y. Li, K. Jiang, X. Wang, Photophysical, G-quadruplex DNA binding and cytotoxic properties of terpyridine complexes with a naphthalimide ligand, *RSC Adv.* 6 (2016) 36923–36931.
- [34] D. Dong, Z. Li, D. Liu, N. Yu, H. Zhao, H. Chen, J. Liu, D. Liu, Postsynthetic modification of single Pd sites into uncoordinated polypyridine groups of a MOF as the highly efficient catalyst for Heck and Suzuki reactions, *New J. Chem.* 42 (2018) 9317–9323.
- [35] D. Pérez, E. Guitián, Selected strategies for the synthesis of triphenylenes, *Chem. Soc. Rev.* 33 (2004) 274–283.
- [36] S. Kumar, Self-organization of disc-like molecules: chemical aspects, *Chem. Soc. Rev.* 35 (2006) 83–109.
- [37] S. Sergeyev, W. Pisula, Y.H. Geerts, Discotic liquid crystals: a new generation of organic semiconductors, *Chem. Soc. Rev.* 36 (2007) 1902–1929.
- [38] K. Togashi, S. Nomura, N. Yokoyama, T. Yasuda, C. Adachi, Low driving voltage characteristics of triphenylene derivatives as electron transport materials in organic light-emitting diodes, *J. Mater. Chem.* 22 (2012) 20689–20695.
- [39] M. Iwasaki, S. Iino, Y. Nishihara, Palladium-catalyzed annulation of o-iodobiphenyls with o-bromobenzyl alcohols: synthesis of functionalized triphenylenes via C-C and C-H bond cleavages, *Org. Lett.* 15 (2013) 5326–5329.
- [40] H. Jiang, Y. Zhang, D. Chen, B. Zhou, Y. Zhang, An approach to tetraphenylenes via Pd-catalyzed C-H functionalization, *Org. Lett.* 18 (2016) 2032–2035.
- [41] S. Pan, H. Jiang, Y. Zhang, D. Chen, Y. Zhang, Synthesis of triphenylenes starting from 2-iodobiphenyls and iodobenzenes via palladium-catalyzed dual C-H activation and double C-C bond formation, *Org. Lett.* 18 (2016) 5192–5195.